Elastic and inelastic scattering of 291-MeV pions by ^{9}Be, Si, ^{58}Ni, and ^{208}Pb

D. F. Geesaman, C. Olmer,* and B. Zeidman
Argonne National Laboratory, Argonne, Illinois 60439

R. L. Boudrie
University of Colorado, Boulder, Colorado 80302
and Los Alamos Scientific Laboratory, Los Alamos, New Mexico 87544

G. S. Blanpied,† M. J. Devereux,‡ and G. R. Burleson
New Mexico State University, Las Cruces, New Mexico 88001

R. E. Segel
Northwestern University, Evanston, Illinois 63301

L. W. Swenson
Oregon State University, Corvallis, Oregon 97331

H. A. Thiessen
Los Alamos Scientific Laboratory, Los Alamos, New Mexico 87545
(Received 24 November 1980)

Angular distributions for the elastic and inelastic scattering of 291-MeV π^+ and π^- by ^{9}Be, Si, ^{58}Ni, and ^{208}Pb have been measured. The characteristics of two first-order optical potentials have been investigated, and reasonable agreement with the elastic scattering data has been obtained. Macroscopic distorted-wave impulse approximation calculations of the inelastic scattering with Kisslinger potentials are reasonably successful in reproducing the experimental data. The inelastic scattering results for ^{9}Be provide evidence for the importance of radial localization effects in pion inelastic scattering.

[NUCLEAR REACTIONS ^{9}Be(π, π'), Si(π, π'), ^{58}Ni(π, π'), ^{208}Pb(π, π'), $E_\pi = 291$ MeV, measured $d\sigma/d\Omega$; optical potential and DWIA collective analyses.]

I. INTRODUCTION

A large body of experimental information has now been accumulated on pion scattering from nuclei at energies well below and near the $J = T = \frac{3}{2}$, $\Delta(1232)$ pion-nucleon resonance.[1] However, relatively few data are available at pion kinetic energies above 250 MeV. Since the P_{33} resonance introduces a strong energy dependence into the elementary pion-nucleon amplitude, it is important to have high-quality data over a wide range of incident energies to adequately test models of pion-nucleus interactions in regimes where the pion is either weakly or strongly absorbed. In addition, this strong energy dependence allows the possibility of selectively studying the radial dependence of nuclear structure effects in pion reactions.

The present work reports a study of scattering of both π^+ and π^- by ^{9}Be, Si, ^{58}Ni, and ^{208}Pb at an incident energy of 291 MeV. The elastic scattering data are discussed in the context of two simple first-order optical potentials. Satisfactory agreement between the optical-model calculations and the data can be obtained for all targets except ^{9}Be, but only at the expense of modifying parameters of the calculations. Inelastic scattering data for low-lying collective transitions have been analyzed in terms of the distorted-wave impulse approximation. Within the framework of a phenomenological parametrization, reasonable agreement is obtained with the results of other hadronic probes. This analysis, together with that reported previously for the same targets at $E_\pi = 162$ MeV,[2] completes a survey of pion scattering from a broad range of nuclei at energies on and above the P_{33} resonance energy. The present analysis is guided by the spirit and experience of the previous work.

II. EXPERIMENTAL PROCEDURE

The experiment was performed on the EPICS system[3] at the Clinton P. Anderson Meson Physics Facility. The incident pion energy was 291.2 MeV, nearly the highest energy available from the EPICS channel. Because of saturation effects in the channel magnets, the system resolution was only ~600 keV. However, this was adequate for resolving the ground state and first-excited state

for each of the present targets. The central 2° of the spectrometer acceptance was divided into two 1° bins for the elastic scattering analysis. To improve the statistical significance of the inelastic data, the full 2° acceptance was used. The π^+ scattering data were measured from 10° to 84° in 2° steps and the π^- data were measured from 10° to 78°. The angular resolution was better than 1°, and the absolute angle calibration was known to better than 0.2°.

Targets of ^{9}Be (160 mg/cm^2), isotopically enriched ^{58}Ni (292 mg/cm^2) and ^{208}Pb (289 mg/cm^2), and natural Si (360 mg/cm^2) were used. Typical energy spectra for π^+ scattering from these targets are shown in Fig. 1. The relative normalization of the data was provided by measuring the flux in two ion chambers situated at 0° downstream of the target. An alternative normalization based on the total yield at the production target was also employed. The two methods were found to be consistent throughout the experiment. Measurements were repeated at several angles whenever changes were made in the configuration of the channel or spectrometer. The absolute normalization was obtained by a comparison to the scattering from hydrogen at two angles (θ_{lab}=42.0° and 52.5°); the hydrogen cross sections were obtained from the work of Bussey *et al.*[4] The uncertainty in the absolute cross sections in the present work is estimated to be less than ±10%, while the relative cross sections are believed to be determined to ±5%, ignoring purely statistical errors. No corrections due to radiative effects have been applied to the present data. They are estimated to be considerably smaller than the statistical uncertainties for the data considered here.[5]

III. EXPERIMENTAL RESULTS

The angular distributions for the elastic scattering of 291 MeV π^+ and π^- are shown in Figs. 2 and 3. These angular distributions are much smoother than those observed on the same targets at 162 MeV where the angular distributions exhibit very strong oscillations with equal minima depths for both π^+ and π^-. At 291 MeV, the minima in the angular distributions of the even-even targets are considerably deeper for π^- scattering than for π^+ scattering. As Germond and Wilkin have pointed out, this is a result of the differences in the relative phases of the Coulomb and nuclear amplitudes at the two energies.[6]

Qualitatively, an estimate of the interaction radius can be obtained in a strong absorption limit.[7] The oscillation pattern is given by $J_1^2(qR)$, where q is the momentum transfer, R is an effective radius ($R \sim R_{\text{nucleus}} + \lambda\!\!\!^{-}_{\pi}$, where $\lambda\!\!\!^{-}_{\pi}$ is the reduced pion wavelength), and J_1 is the Bessel function of order one. The locations of the first minima imply that the effective radii are

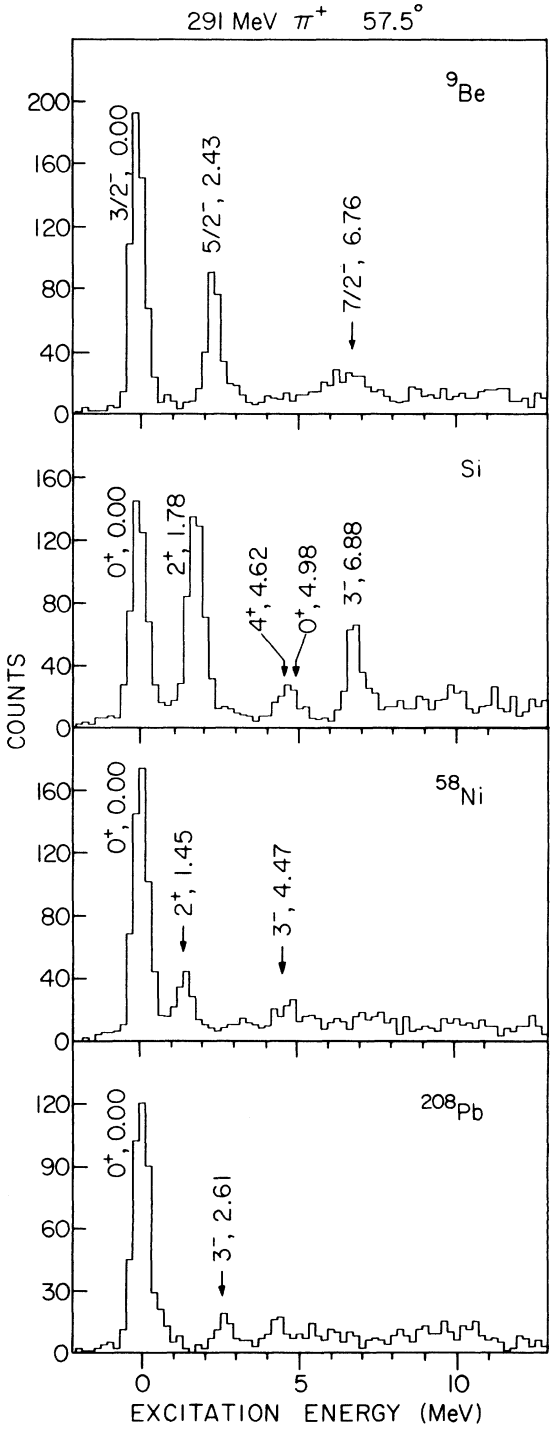

FIG. 1. Energy spectra obtained for the scattering of 291 MeV π^+ by ^{9}Be, Si, ^{58}Ni, and ^{208}Pb at a laboratory angle of 57.5°.

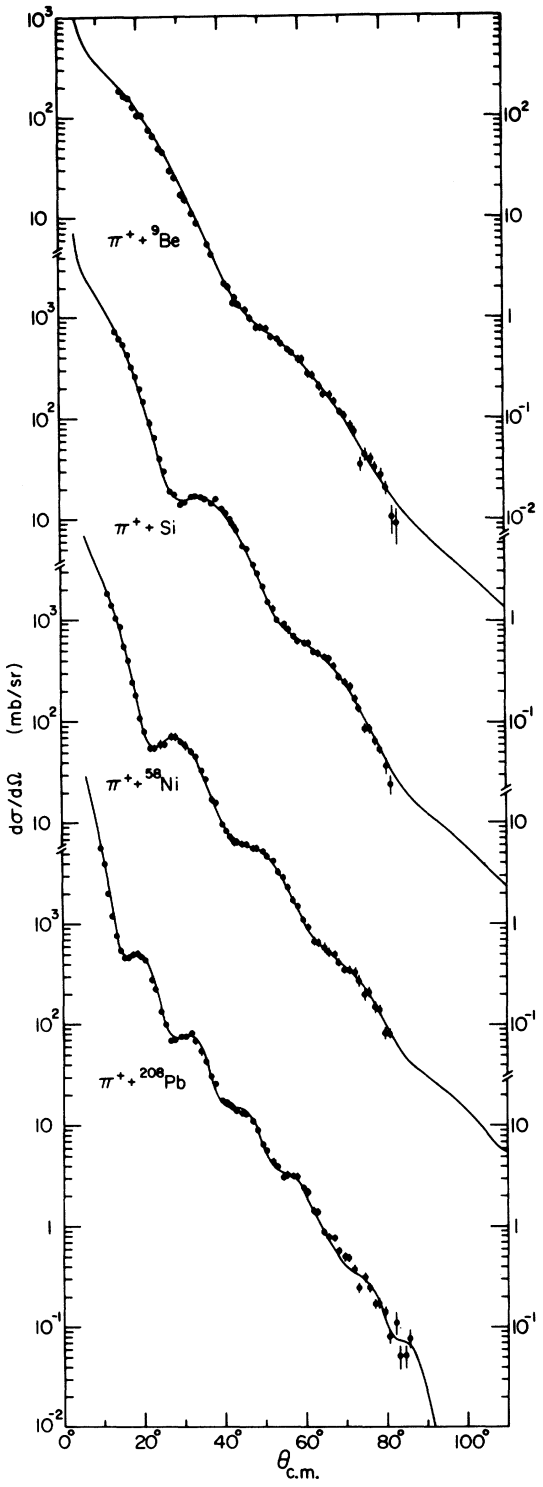

FIG. 2. Angular distributions for the elastic scattering of 291 MeV π^+ by ^{9}Be, Si, ^{58}Ni, and ^{208}Pb. The curves result from fits to the data using Kisslinger optical potentials.

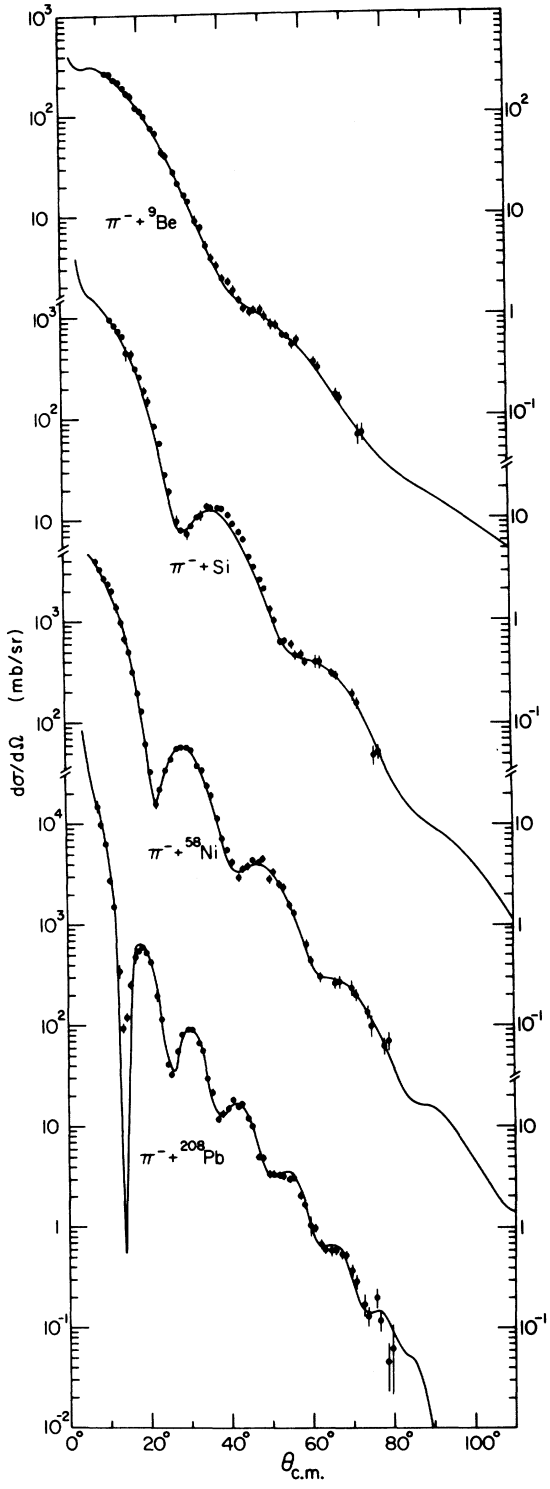

FIG. 3. Angular distributions for the elastic scattering of 291 MeV π^- by ^{9}Be, Si, ^{58}Ni, and ^{208}Pb. The curves result from fits to the data using Kisslinger optical potentials.

approximately 0.7 fm larger than the half-density radii, and roughly 0.6 fm smaller than the effective radii at 162 MeV.[2] The difference in reduced wavelength can only account for a 0.25 fm change in the effective radius. The remaining difference can be compared with an estimated 0.7 fm difference in the pion mean-free path for the two energies. (The mean-free path was taken to be $2/[\rho_N(\sigma_{\pi^+N}+\sigma_{\pi^-N})]$, where ρ_N is the density of nuclear matter and σ_{π^+N} and σ_{π^-N} are the pion-nucleon total cross sections.) Such an argument suggests that the 291-MeV π-nucleus interactions occur at roughly the half-density radius, a significantly deeper penetration of the nucleus than at 162 MeV.

While such qualitative considerations may be useful in establishing the scale of pion-nucleus interactions, a more detailed understanding can be obtained only with the introduction of a model. In the following section we describe optical-model calculations of the elastic scattering. In Sec. III A, a Kisslinger form[8] is assumed for the optical potential while in Sec. III B, a static model of Landau, Phatak, and Tabakin (LPT)[9] is employed. The subject of pion nucleus optical potentials has received considerable theoretical attention in recent years. It is clear that higher-order effects such as true pion absorption must be included for a complete description of the interaction.[10] (True absorption is defined as the process in which no pions are present in the outgoing channel, so as to distinguish this process from optical model absorption, where the pion no longer remains in the elastic entrance channel.) The use of two first-order models can still be defended as a means of providing a useful parametrization of the experimental data. It is in the spirit of this type of phenomenology that the optical-model calculations are performed. Whether such a phenomenology can simultaneously reproduce both the elastic and inelastic data at several energies is still an open question. One of the conclusions of Ref. 2 was that such an approach was effective for 162-MeV pion-nucleus interactions.

The analysis of pion scattering from ^{9}Be is complicated by the structure of the ^{9}Be target nucleus. In particular, a significant quadrupole contribution to the elastic scattering at 162 MeV has been observed.[11] Since this is related to quadrupole inelastic transitions, a discussion of the elastic and inelastic scattering from ^{9}Be will be given separately in Sec. V.

A. Kisslinger optical potential

The elastic scattering data from the even-even targets were fit with an optical potential of the Kisslinger form:

$$2EV(\bar{r}) = -Ak^2 b_0 \rho(\bar{r}) + A b_1 \nabla \cdot \rho(\bar{r}) \nabla , \quad (1)$$

where $\rho(\bar{r})$ is the nuclear matter density. The complex parameters b_0 and b_1 were adjusted to obtain a least-squares fit to the data. The parameters of the charge distributions were taken from electron scattering results.[12] The matter distributions were assumed to be of Woods-Saxon form, with identical neutron and proton distributions. To correct for the proton charge form factor, the parameters of the matter distributions were obtained by adjusting the half-density radii so that the mean square matter radii were 0.64 fm^2 less than the mean square charge radii. The π^+ and π^- data were treated independently. The calculations were performed with the computer code FITPI,[13] and the resulting best-fit parameters are presented in Table I. In separate fits, the overall normalization of each data set was allowed to vary. In all cases, the resulting "optimum normalizations" were within 13% of the experimentally established normalizations, and the improvements in the quality of the fits were minimal.

The final calculations are shown as the solid curves in Figs. 2 and 3. These fits are in excellent agreement with the experimental angular distributions, as evidenced by the rather good χ^2 values in Table I. For Si and for ^{58}Ni, the best fit parameters for π^+ and π^- scattering are reasonably consistent, while there are large differences in both $\mathrm{Re}(b_0)$ and $\mathrm{Re}(b_1)$ between the π^+ and π^- results for ^{208}Pb. These ^{208}Pb differences can be interpreted as a measure of the isospin dependence of the optical potential. Due to continuous ambiguities in the parameters, it is not possible to separately extract the isospin dependence of each term in the potential. The Kisslinger parameters corresponding to the isospin averaged ($N=Z$) free pion-nucleon phase shifts are also listed in Table I. No corrections for Fermi averaging have been applied, and such corrections were calculated to be small at this energy.[14] The most significant differences between the free-nucleon and fitted parameters are that the fitted magnitudes of $\mathrm{Im}(b_1)$ and $\mathrm{Re}(b_0)$ are generally much larger than the free-nucleon values and that the fitted value of $\mathrm{Re}(b_1)$ is much smaller than the free nucleon value. [For $\pi^- + ^{208}$Pb the final $\mathrm{Re}(b_0)$ and $\mathrm{Re}(b_1)$ agree with the free nucleon values.] Since the pion is absorbed in the surface region, the result for $\mathrm{Re}(b_0)$ and $\mathrm{Re}(b_1)$ may be affected by a continuous ambiguity in the real potential. This was checked by fixing $\mathrm{Re}(b_0)$ to the free value. These 3-parameter fits did result in values of $\mathrm{Re}(b_1)$ nearer the free

TABLE I. Optical-potential parameters used in the FITPI calculations.

Nucleus	Data	R_{ch}[a] (fm)	a_{ch}[a] (fm)	R[a] (fm)	a[a] (fm)	Re(b_0)[b] (fm^3)	Im(b_0)[b] (fm^3)	Re(b_1)[b] (fm^3)	Im(b_1)[b] (fm^3)	χ^2/point	$\sigma_{elastic}$ (mb)	$\sigma_{reaction}$ (mb)
^{9}Be	π^+	2.03	0.53	1.75	0.53	0.2±0.2	1.0±0.2	−2.8±0.3	2.1±0.2	0.9	119	224
	π^-	2.03	0.53	1.75	0.53	1.75±0.3	1.7±0.2	−4.9±0.4	1.9±0.2	0.7	135	242
^{9}Be $L=0$	π^+	2.03	0.53	1.75	0.53	0.0±0.2	1.3±0.1	−1.1±0.2	2.7±0.2	0.8	116	274
	π^-	2.03	0.53	1.75	0.53	2.5±0.8	1.6±0.2	−2.0±0.5	3.1±0.2	0.7	123	310
Si	π^+	3.11	0.55	2.82	0.55	−1.7±0.2	0.1±0.2	0.0±0.2	4.3±0.2	0.7	389	549
	π^-	3.11	0.55	2.82	0.55	−1.5±0.2	0.4±0.2	−0.3±0.2	3.5±0.2	0.6	396	558
^{58}Ni	π^+	4.08	0.54	3.97	0.54	−1.9±0.2	0.1±0.2	0.4±0.2	3.9±0.2	0.8	649	831
	π^-	4.08	0.54	3.97	0.54	−1.6±0.2	0.3±0.2	−0.3±0.2	3.2±0.2	1.0	701	864
^{208}Pb	π^+	6.62	0.55	6.51	0.55	−1.1±0.3	0.2±0.2	0.2±0.4	3.9±0.2	1.5	1494	1791
	π^-	6.62	0.55	6.51	0.55	0.3±0.5	0.6±0.3	−2.7±0.3	3.4±0.3	2.4	1926	2014
Free pion-nucleon parameters[c]				E_π = 291 MeV		−0.45	0.26	−2.0	2.2			
				E_π = 250 MeV		−0.53	0.28	−2.4	3.7			

[a] The density distributions were assumed to have a Woods-Saxon form:

$$\rho(r) = [3A/4\pi(R^3 + \pi^2 a^2 R)]/(1 + \exp[(r-R)/a]).$$

The parameters R_{ch} and a_{ch} characterize the charge density while the parameters R and a characterize the matter density.

[b] These parameters were varied during the fit.

[c] Isospin averaged for a $T=0$ target such as ^{28}Si, Ref. 14.

nucleon value, with no change in Im(b_1). While the quality of these fits was acceptable, the χ^2 values for these last fits were roughly a factor of 2 worse than those of the 4-parameter fits.

The more significant difference between the fitted and free values is the consistently large fitted value of the Im(b_1). Phenomenologically, the best-fit values of Im(b_1) seem to correspond to free-nucleon values for pion energies of ~250 MeV. Since the present energy is well above the resonance, it might be expected that Fermi averaging would reduce the average π-nucleon interaction energy. However, the calculations of Ref. 14 do not show such a shift. This question will be discussed further below.

In conculsion, the present elastic scattering data can be well reproduced by optical potentials of the Kisslinger form with adjustable parameters. The fitted parameters are, however, rather different than the free pion-nucleon values. In particular, the large p-wave absorption seems to be more characteristic of a pion energy of 250 MeV than of 291 MeV. Inelastic scattering calculations based on deforming the potentials obtained here are presented in Sec. IV.

B. LPT optical potential

The first order LPT potential is a more microscopic approach to the pion-nucleus potential. The impulse approximation (as in the Kisslinger model) relates the potential to the pion-nucleon amplitude. On-shell, the free pion-nucleon amplitude is used. By performing the calculation in momentum space, it is more natural to include a realistic off-shell extrapolation.[15] The nuclear matter distributions were assumed to be of Woods-Saxon form and the effect of nucleon Fermi motion was neglected. The momentum space elastic scattering code PIPIT (Ref. 16) was used to perform the calculations.

In the impulse approximation, the energy in the π-nucleon system is essentially a free parameter[17] which is generally assumed to be near the Lorentz-transformed value of the π-nucleus energy. In Ref. 2, substantial improvement of the quality of the fits was obtained if this energy was shifted to account for Coulomb and binding effects. Since the reaction occurs at the nuclear surface and the pion interacts primarily with the valence nucleons, known separation energies and surface Coulomb energies were used. While these adjustments seem physically reasonable, and have some theoretical basis,[18] it must be emphasized that at 291 MeV they represent essentially free parameters.

In Figs. 4 and 5, the results of calculations (solid curves) assuming the same matter distributions as in the previous section together with the Coulomb and binding corrections of Ref. 2 are compared to the data. The parameters used in these calculations are tabulated in Table II. Clearly, the slope of the calculation is incorrect in each case. At 162 MeV, it was observed that agreement with experiment could be obtained with

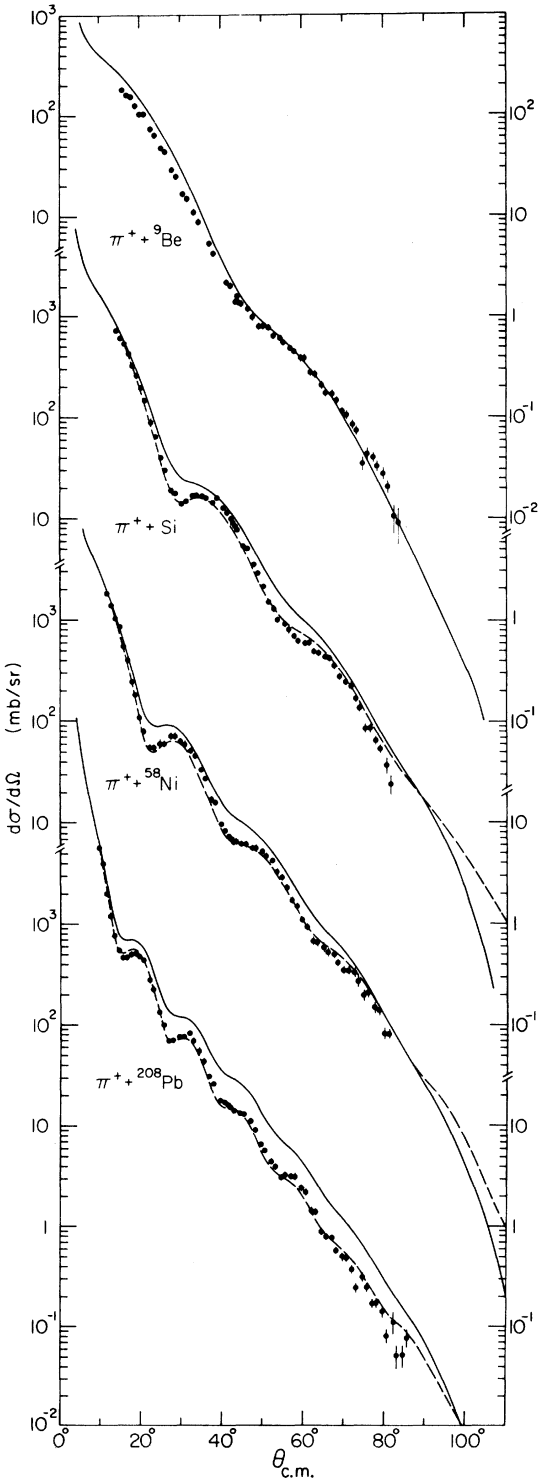

FIG. 4. Angular distributions for the elastic scattering of 291 MeV π^+ by ^{9}Be, Si, ^{58}Ni, and ^{208}Pb. The curves result from optical-potential calculations using LPT optical potentials assuming matter distributions (Table II) deduced from electron scattering studies (solid lines) and matter distributions (Table III) modified from these values (dashed lines).

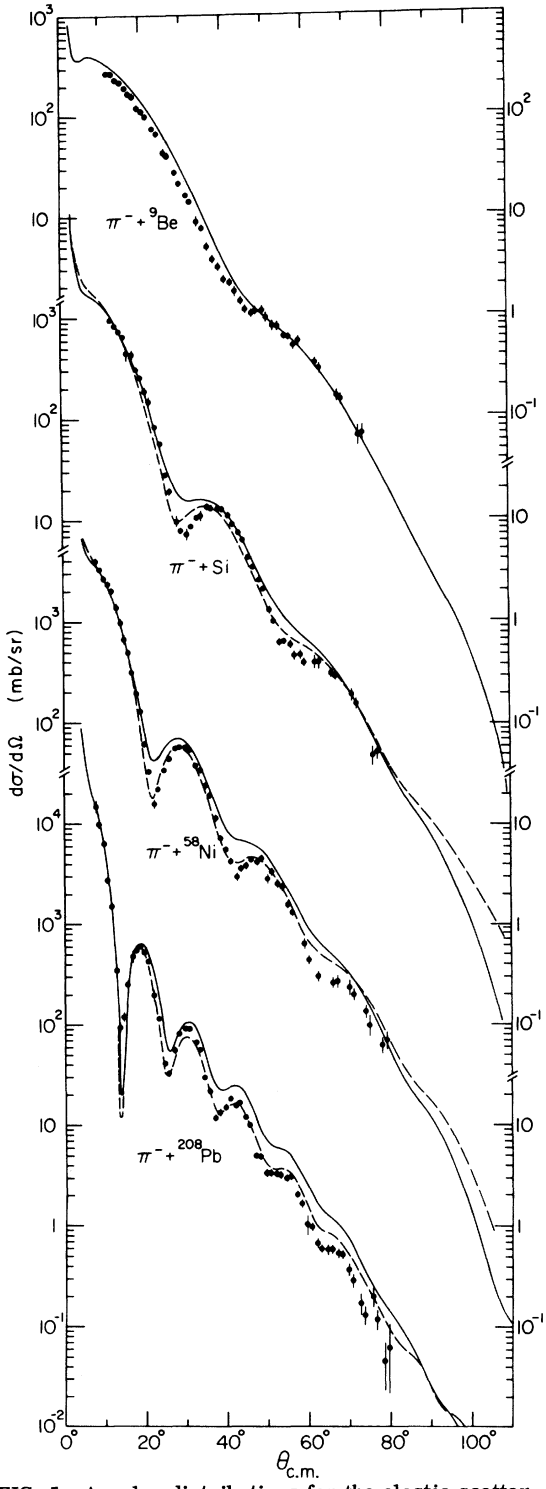

FIG. 5. Angular distributions for the elastic scattering for 291 MeV π^- by ^{9}Be, Si, ^{58}Si, and ^{108}Pb. The curves result from optical-potential calculations using LPT optical potentials, assuming matter distributions (Table II) deduced from electron scattering studies (solid lines) and matter distributions (Table III) modified from these values (dashed lines).

TABLE II. Optical-model parameters obtained from electron scattering used in the LPT calculations of the solid curves on Figs. 4 and 5.

	Beam	R (fm)	a (fm)	ΔE_{Coul}[a] (MeV)	$\Delta E_{\text{binding}}$[a] (MeV)
^{9}Be	π^+	1.75	0.53	1.52	13.1
	π^-	1.75	0.53	−1.52	5.5
Si	π^+	2.82	0.55	3.89	13.0
	π^-	2.82	0.55	−3.89	15.8
^{58}Ni	π^+	3.97	0.54	6.32	11.8
	π^-	3.97	0.54	−6.32	10.4
^{208}Pb	π^+	6.51	0.55	12.65	7.8
	π^-	6.51	0.55	−12.65	7.5

[a] Taken from Ref. 2.

this potential only if the nuclear geometries were modified. By varying the radius, diffuseness, and binding energy correction in a grid search procedure, considerably better agreement with the 291-MeV data was obtained. These calculations are displayed as the dashed curves in Figs. 4 and 5, and use the parameters given in Table III. In each case, relative to Table II, it was necessary to increase the diffuseness parameter a, to give the correct slope, and to substantially increase the binding correction to obtain sufficiently deep minima.

While these substantial changes in the matter distributions and binding energies are required empirically to fit the data, the interpretation of such changes is difficult. Presumably, the adjustments correct for deficiencies in the underlying model. Several important effects have been neglected in this version of the LPT potential, most notably true pion absorption. It is interesting to note that the required changes in rms. radii are nearly the same at 162 and 291 MeV. It has been suggested[19] that these modifications are a reflection of the relatively long range inherent in the off-shell extrapolation of Ref. 15. Further investigations of these off-shell effects are certainly necessary.

TABLE III. Optical model parameters used in the LPT calculations which were adjusted to fit the experimental elastic angular distributions The results of these calculations are shown in the dashed curves in Figs. 4 and 5.

	Beam	R[a] (fm)	a[a] (fm)	ΔE_{coul}[b] (MeV)	$\Delta E_{\text{binding}}$[a] (MeV)
^{9}Be	π^+	1.5	0.45	1.5	50
$L=0$	π^-	1.6	0.45	−1.5	50
Si	π^+	2.2	0.63	3.9	50
	π^-	2.2	0.63	−3.9	50
^{58}Ni	π^+	3.4	0.60	6.3	50
	π^-	3.3	0.63	−6.3	50
^{208}Pb	π^+	6.0	0.65	12.6	50
	π^-	6.0	0.68	−12.6	40

[a] Varied in the calculations.
[b] Held fixed at the values of Ref. 2.

It is also interesting that the size of the binding energy corrections required here are approximately the same as those required to obtain the correct value of $\text{Im}(b_1)$ with free π-nucleon amplitudes in the Kisslinger potential. The justification for the large binding correction may be better understood. Partly, it may be due to the increased penetration of the nucleus at 291 MeV, since as the pion penetrates further into the nucleus, the average binding energy per particle will increase. Indeed, calculations of quasifree electron scattering require average potential energies of ~40 MeV to account for the observed spectral shapes.[20] However, for the pionic case, the absorption is still sufficiently strong that it seems very unlikely that the pion samples the entire nuclear interior. The binding correction may also be partially explained as a consequence of nucleon Fermi motion. Since the average π-nucleon energy is well above resonance, the energy dependence of the pion-nucleon amplitudes will favor interactions in which the nucleon Fermi motion is directed away from the incident pion, thereby lowering the energy in the π-nucleon system. This can be experimentally observed in the kinetic energy spectra for pion inelastic scattering at 291 MeV where, at back angles, the centroid of the energy spectrum is ~30 MeV lower than the free π-nucleon kinematic value.[1,21] However, this is not in agreement with the theoretical results of Ref. 14, which suggested that Fermi averaging did not significantly change the Kisslinger model parameters at this energy.

In conclusion, reasonable agreement can be obtained with the experimental data if large modifications are made to the measured matter distributions and large binding energy corrections are included. These modifications are only sensible in a phenomenological approach, and signal serious deficiencies in the underlying model.

IV. INELASTIC SCATTERING

Inelastic scattering is another important aspect of the interactions of pions with nuclei. In a phenomenological approach it is expected that both elastic and inelastic scattering will be described in the same framework. This consistency condition may provide more information on the

pion-nucleus potential and is essential before reliable nuclear structure information can be extracted.

In the present work, the relatively poor resolution limited the analysis of inelastic scattering to the strong collective states. Angular distributions for the inelastic scattering of π^+ and π^- by ^{9}Be (2.4 MeV, $\frac{5}{2}^-$; 6.8 MeV, $\frac{7}{2}^-$), ^{28}Si (1.8 MeV, 2^+; 4.6+5.0 MeV, 4^++0^+, 6.9 MeV, 3^-+4^+), ^{58}Ni(1.5 MeV, 2^+; 4.5 MeV, 3^-), and ^{208}Pb (2.6 MeV, 3^-) are presented in Figs. 6–9. With the present resolution, the determination of inelastic yields is subject to significant errors that result from the tail of the elastic peak and the possible presence of weakly excited unresolved states. Such errors are, of course, more important in regions of relative minima of the angular distributions than near relative maxima.

Previous studies have investigated inelastic scattering on ^{9}Be at 162 MeV,[11] on ^{28}Si at 130, 162, 180, and 226 MeV,[2,22] on ^{58}Ni at 162 MeV,[2] and on ^{208}Pb at 80, 115, and 162 MeV.[2,23]

The experimental angular distributions displayed in Figs. 6–9 are generally smooth, without well-defined minima. The π^+ and π^- angular distributions are similar in all cases except for ^{208}Pb, where a shift in the locations of the maxima is observed. This shift is comparable to that seen in the elastic scattering data and, as is shown below, results from Coulomb effects.

The inelastic scattering of π^+ and π^- has been calculated on the basis of the distorted wave impulse approximation (DWIA) and a macroscopic form factor which directly relates the inelastic

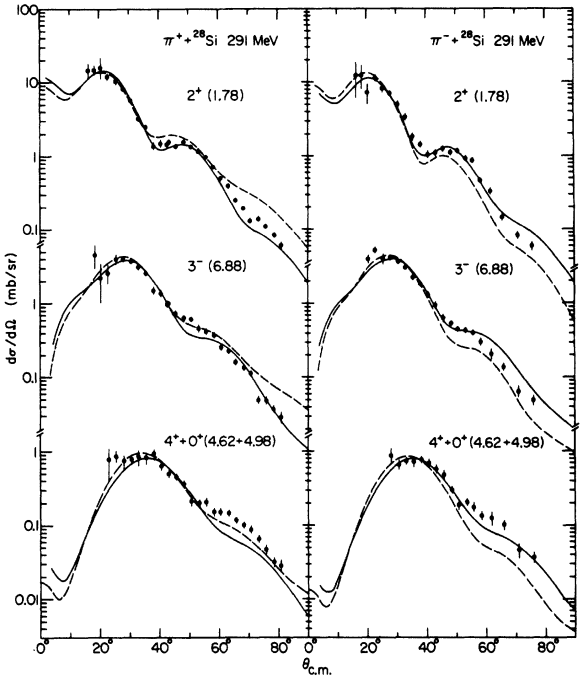

FIG. 7. Angular distributions for the inelastic scattering of 291 MeV π^+ and π^- to the 2^+, 1.78-MeV and 3^-, 6.88-MeV, states and the 4^+, 4.62 MeV and 0^+, 4.98-MeV doublet in ^{28}Si. The curves result from collective DWIA calculations with Kisslinger (solid) and LPT (dashed) optical potentials. The curves for 4.62 doublet assume only an $L=4$ contribution, while the curves for the 6.88-MeV doublet assume only an $L=3$ contribution.

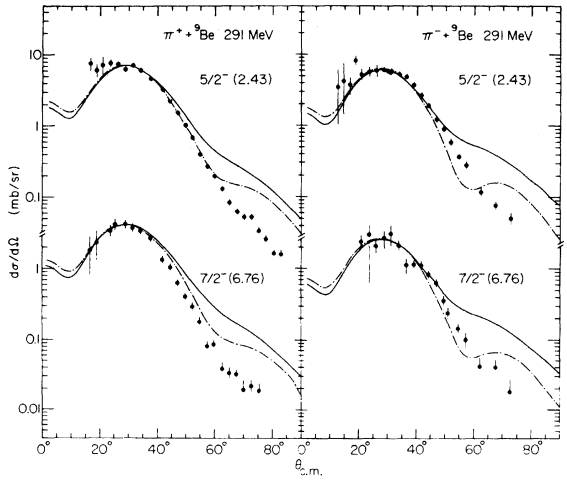

FIG. 6. Angular distributions for the inelastic scattering of 291 MeV π^+ and π^- to the $\frac{5}{2}^-$, 2.43-MeV and $\frac{7}{2}^-$ 6.76-MeV states in ^{9}Be. The curves result from DWPI calculations with the optical parameters fitted to the ^{9}Be elastic data (solid) and with optical model parameters fitted to the ^{9}Be $L=0$ elastic data (dot-dash).

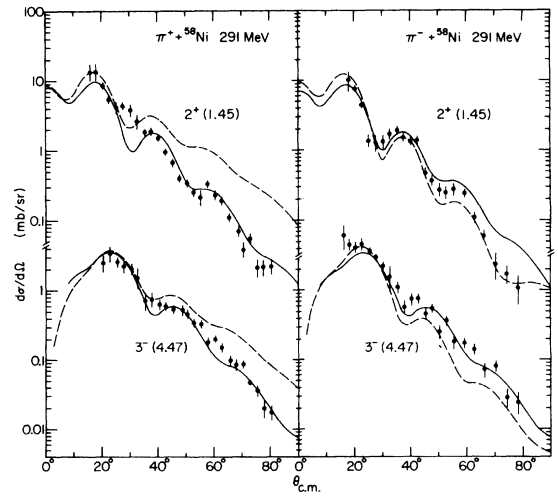

FIG. 8. Angular distributions for the inelastic scattering of 291 MeV π^+ and π^- to the 2^+, 1.45 and 3^-, 4.47-MeV states in ^{58}Ni. The curves result from collective DWIA calculations with Kisslinger (solid) and LPT (dashed) optical potentials.

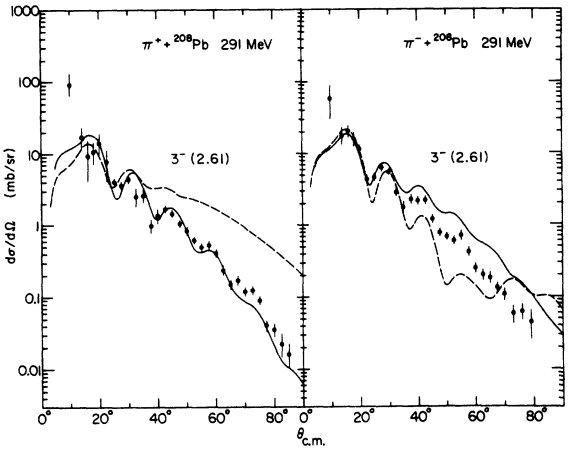

FIG. 9. Angular distributions for the inelastic scattering of 291 MeV π^+ and π^- to the 3^-, 2.61-MeV state in ^{208}Pb. The curves result from collective DWIA calculations with Kisslinger (solid) and LPT (dashed) optical potentials.

scattering to deformation of the elastic optical potential

$$\langle \phi_{I'M'} | H | \phi_{IM} \rangle = \frac{A t_{\pi N} \beta_L r}{2L+1} \frac{d\rho(r)}{dr}, \tag{2}$$

where L is the transferred orbital angular momentum, A is the atomic weight of the target, $t_{\pi N}$ is the π-nucleon t-matrix, and β_L is the deformation parameter. Calculations were carried out both with the Kisslinger and the LPT potentials, using the parameters of Tables I and III, respectively. The resulting deformation parameters, determined by visually adjusting the calculations to reproduce the experimental data, are listed in Table IV. Calculations with the Kisslinger potential were performed with the code DWPI,[24] while the calculations with the LPT potential were carried out with the program of Lee and Chakravarti (LC).[25] The final calculations are shown as the solid (DWPI) and dashed (LC) curves on Figs. 6–9. Since we have modified the nuclear density distributions to fit the elastic scattering data, there is some question regarding the density distribution to be used in an inelastic calculation [Eq. (2)]. Here we have chosen to use the same density distribution as in the elastic calculations. The result of using a larger density radius is essentially to give the same angular distribution scaled by the radius, i.e., the usual βR ambiguity.

The DWPI calculations give a reasonable representation of the data in each case. However, the slope of the angular distribution is not correctly given for the π^- scattering to the Pb 3^- state and, to a lesser extent, for the ^{58}Ni 2^+ state. The deformation lengths (βR) agree well with those obtained at 162 MeV[2] and those obtained with other probes.

The LC calculations also provide a reasonable description of the data for π^+ and π^- inelastic scattering on ^{28}Si. For ^{58}Ni and ^{208}Pb, however, the calculated π^+ cross sections fall too slowly with angle. The calculated π^- angular distribution for the ^{208}Pb 3^- state is in significant disagreement with the data. The source of this discrepancy is not understood and it makes the extraction of deformation lengths very uncertain for these cases. Given these limitations, the deformation parameters β are relatively consistent for the two approaches, except those for the ^{208}Pb, 3^- state. Since the radii of the LPT potentials are smaller than those of the Kisslinger potentials, the deformation lengths extracted with the Kisslinger potential are larger than those extracted with the LPT potential. However, it is possible that with a nonlocal potential such as the LPT potential, the use of the half-density radius is not appropriate for the comparison of deformation lengths.

V. PION SCATTERING FROM ^{9}Be

For the $J=\frac{3}{2}$ nucleus ^{9}Be, the approach of the previous sections may be incomplete. The large quadrupole moment of the ^{9}Be ground state suggests that quadrupole ($L=2$) as well as scalar ($L=0$) interactions are important in the elastic scattering. Indeed, at 162 MeV, the analysis of both π^+ and π^- scattering indicated that the quadrupole contribution was significant and was required for adequate agreement with the data. The angular distributions for ^{9}Be did not show strong oscillations, in marked contrast to the data on even-even targets, and the quadrupole scattering provided a mechanism for filling in the minima. In addition, the relative inelastic scattering cross sections for the $\frac{5}{2}^-$ and $\frac{7}{2}^-$ states were also reproduced in a strong coupling rotational model. In the rotational model limit, Blair and Naqib[36] have shown, by means of the adiabatic approximation, that the cross section to any member of the ground-state rotational band is

$$\frac{d\sigma}{d\Omega}(I \to I') = \delta_{I,I'} \frac{d\sigma}{d\Omega}(L=0) + \sum_{L \neq 0} \langle IKL0 | I'K \rangle^2 \frac{d\sigma}{d\Omega}(L). \tag{3}$$

In this expression, $I(I')$ is the initial (final) state spin and $(d\sigma/d\Omega)(L=0)$ and $(d\sigma/d\Omega)(L\neq 0)$ are the elastic and in-band inelastic cross sections for scattering from a spin zero target whose intrinsic deformation and optical parameters are the same

as those of the odd-mass nucleus in its rotational band. The measured inelastic cross sections can therefore be used to determine the part of the cross section due to the scalar and quadrupole interactions.

For the data at 291 MeV, the need for the $L=2$ contribution is much less apparent. The elastic scattering data are fit quite well with a Kisslinger potential, although with parameters which are somewhat different from those obtained for the other targets. (See Figs. 2 and 3 and Table I.) This was also found to be true at 162 MeV. However, a new feature is that calculations with the LPT potential, and matter distributions derived from electron scattering also give a reasonable description of the shape of the angular distributions, as evidenced by the solid curves in Figs. 4 and 5. In addition, the ratio of the inelastic cross section of the $\frac{5}{2}^-$ state to that of the $\frac{7}{2}^-$ state, while consistent with Eq. (3) for π^+ scattering, is not consistent with Eq. (3) for π^- scattering; i.e., the ratio is too large by a factor of ~1.8.

Except for π^- scattering to the $\frac{7}{2}^-$ state, inelastic scattering calculations with the Kisslinger potential (solid curves in Fig. 6) give values of β in agreement with those obtained at 162 MeV and suggest that the collective approach may be valid (Table IV). Proceeding on this assumption, Eq. (3) can be used to subtract the quadrupole contribution and obtain the ^{9}Be $L=0$ elastic scattering data shown in Fig. 10. The cross sections for π^+ and π^- inelastic scattering to the $\frac{5}{2}^-$ state were used to determine $(d\sigma/d\Omega)(L=2)$. These subtracted data were then fit with the Kisslinger and LPT optical potentials. The results are shown in Fig. 10 with the parameters given in Tables I and III. DWPI calculations using these Kisslinger parameters are shown as the dot-dashed curves in Fig. 6. They do somewhat better in describing the shapes of the inelastic angular distributions than do the calculations with optical parameters fit to the measured elastic data. The deformation parameters differ by only 5–10% for the two sets of calculations. This does not offer a clear answer to the question of the importance of the quadrupole term in the elastic scattering.

The results with the LPT potential are more disturbing. A reasonable fit to the measured data was obtained using electron scattering density parameters and a very small binding correction. A better fit is obtained if the π^+ data are renormalized by a factor of 1.1 and the π^- data are renormalized by ~1.3. No acceptable fit could be obtained to the quadrupole corrected data; the dashed curves in Fig. 10 are typical. This suggests that quadrupole contributions to the elastic scattering may be much less important at 291 MeV than at 162 MeV.

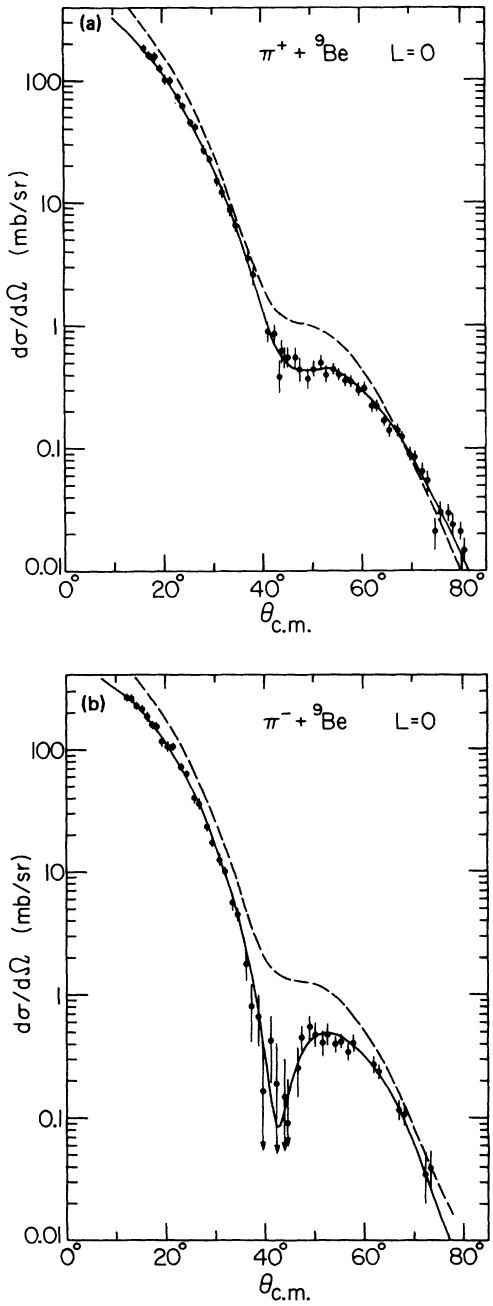

FIG. 10. Angular distributions for the elastic scattering of 291 MeV π^+ (a) and π^- (b) corrected to remove quadrupole contributions through the use of Eq. (3): $(d\sigma/d\Omega)(L=0)=(d\sigma/d\Omega)$ (measured elastic) $-\frac{7}{16}(d\sigma/d\Omega)$ ($\frac{5}{2}^-$, 2.43 MeV). The curves result from optical-model calculations using Kisslinger (solid) and LPT (dashed) optical potentials.

As noted above, the β values for the $\frac{5}{2}^-$ and $\frac{7}{2}^-$ states in π^+ scattering and the $\frac{5}{2}^-$ state in π^- scattering are consistent with the collective model at both 291 and 162 MeV, but the value for π^- scat-

TABLE IV. Deformation parameters from $\pi^{\pm}$ inelastic scattering.

Target	Transition E_{ex} (MeV)	J^{π}	Beam	DWPI β	DWPI βR	LC β	LC βR	(e,e') β	Other probes βR
^{9}Be	2.43	$\frac{5}{2}^{+}$	π^{+}	2.4 ±0.1	4.2 ±0.2			0.88[a]	2.2 – 2.6[a]
			π^{-}	2.1 ±0.1	3.7 ±0.2				
	6.76	$\frac{7}{2}^{-}$	π^{+}	1.6 ±0.1	2.8 ±0.2			0.46[a]	1.2[a]
			π^{-}	1.2 ±0.1	2.1 ±0.2				
^{9}Be	2.43	$\frac{5}{2}^{-}$	π^{+}	2.4 ±0.1	4.2 ±0.2				
$L=0$			π^{-}	2.2 ±0.1	3.9 ±0.2				
	6.76	$\frac{7}{2}^{-}$	π^{+}	1.6 ±0.1	2.8 ±0.2				
			π^{-}	1.2 ±0.1	2.1 ±0.2				
^{28}Si	1.78	2^{+}	π^{+}	0.55±0.06	1.55±0.17	0.45±0.06	0.99±0.13	0.39[b]	1.1 – 1.5[b]
			π^{-}	0.49±0.05	1.38±0.14	0.44±0.06	0.97±0.13		
	4.62	4^{+}	π^{+}	0.28±0.03	0.79±0.09	0.36±0.03	0.79±0.07	0.10[b]	0.95[b]
			π^{-}	0.27±0.03	0.76±0.09	0.35±0.03	0.77±0.07		
	6.88	3^{-}	π^{+}	0.44±0.02	1.24±0.06	0.47±0.03	1.03±0.07		1.41[c]
			π^{-}	0.44±0.02	1.24±0.06	0.49±0.03	1.08±0.07		
^{58}Ni	1.45	2^{+}	π^{+}	0.24±0.02	0.95±0.08	0.20±0.06	0.68±0.20	0.14[d]	0.77 – 1.07[d]
			π^{-}	0.22±0.02	0.87±0.08	0.20±0.03	0.68±0.12		
	4.47	3^{-}	π^{+}	0.20±0.02	0.79±0.08	0.16±0.02	0.54±0.07	0.16[d]	0.60 – 0.89[d]
			π^{-}	0.21±0.02	0.83±0.08	0.18±0.02	0.59±0.07		
^{208}Pb	2.61	3^{-}	π^{+}	0.17±0.01	1.1 ±0.08	0.08±0.04	0.48±0.24	0.12[e]	0.52 – 0.95[e]
			π^{-}	0.15±0.01	0.98±0.08	0.13±0.03	0.78±0.18		

[a] Reference 26, 27.
[b] References 28–31.
[c] Reference 31.
[d] References 32–34.
[e] References 32, 33, 35.

tering to the $\frac{7}{2}^{-}$ state is consistent with the collective model only at 162 MeV. Lee and Kurath[37] have considered a microscopic description of pion scattering from $1p$ shell nuclei. Using $1p$-shell wave functions[38] they find that a strong enhancement of $L=2$, $T=0$ transition amplitudes, similar to that required to fit electromagnetic transition rates, is necessary to reproduce a variety of pion inelastic scattering data. With this modification, they reproduce the 162-MeV results for π^{-} and π^{+} excitation of the $\frac{5}{2}^{-}$ state and π^{+} excitation of the $\frac{7}{2}^{-}$ state, but underpredict the cross sections for π^{-} excitation of the $\frac{7}{2}^{-}$ state by a factor of 2. The dashed curves in Fig. 11 represent their calculations for the 291-MeV inelastic scattering. These absolute predictions do rather well for the $\frac{5}{2}^{-}$ state, and underpredict the cross sections for both π^{+} and π^{-} scattering to the $\frac{7}{2}^{-}$ state by ~40%.

One explanation for the difference between the 291 and 162-MeV results may be the radial structure of the nuclear form factors. A neutron skin is expected for ^{9}Be since the odd neutron is weakly bound, but the strong collective structure is evident in inelastic scattering of a number of probes. The relative importance of the collective and noncollective terms depends on the overlap integral of the pion distorted waves with the radial form factor. Since in Ref. 37 the same radial form factor (a harmonic oscillator radial wave function with $b=1.697$) is used for all states, the energy dependence is the same for each component. However, the collective quadrupole mode is

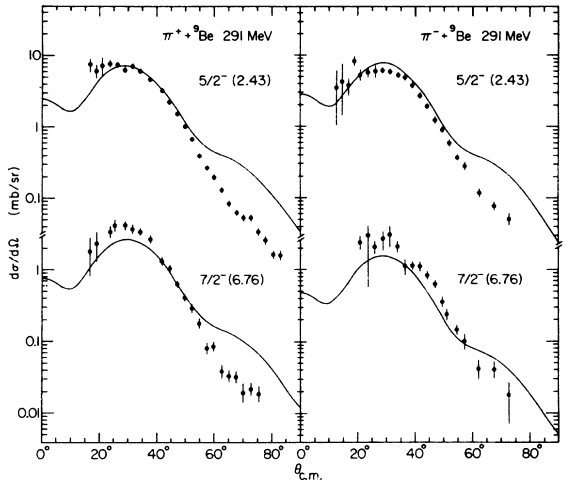

FIG. 11. Angular distributions for the inelastic scattering at 291 MeV π^+ and π^- to the $\frac{5}{2}^-$, 2.43-MeV and $\frac{7}{2}^-$, 6.76-MeV states in ^{9}Be. The curves result from the microscopic DWIA calculations of Lee and Kurath (Ref. 37).

expected to be a surface effect and to have a form factor which may peak at a larger radius than the single particle contributions. At 162 MeV, where the pion is removed from the elastic channel far out in the tail of the nuclear density, one would anticipate that the radial overlap integral would select out only the quadrupole term, thus giving the rotational limit. This is supported by the observation that the β values extracted with pions are roughly a factor of 2 larger than those extracted with other probes. At 291 MeV the pion penetrates more deeply into the nuclear interior, and single particle degrees of freedom can contribute to the inelastic scattering. By varying the energy of the incident pion, one, therefore, may be able to select the region of the radial form factor which contributes to inelastic scattering. The uncertainties in the optical potential, however, signal the need for caution in applying this result. It may be necessary to perform a microscopic calculation of the $L=2$ scattering to the ground state. Possibly interference effects similar to those seen for the $\frac{7}{2}^-$ state may also reduce the relative importance of quadrupole scattering at 291 MeV compared to 162 MeV.

CONCLUSIONS

Elastic and inelastic scattering of both π^+ and π^- by ^{9}Be, Si, ^{58}Ni, and ^{208}Ph has been studied at $E_{\text{lab}}=291$ MeV.[39] The data can be described with a phenomenological approach using Kisslinger potentials when the parameters of the optical potential are varied in order to reproduce the elastic scattering results. The deformation parameters extracted from these calculations are consistent with those obtained from a similar study at 162 MeV and those obtained with other probes. The optical potential parameters seem to be consistent with the free nucleon parameters evaluated at ~40 MeV lower energy.

The calculations with the LPT potential were much less successful. Agreement with the elastic scattering data could be obtained by making significant changes in the matter distributions, as well as introducing a ~50-MeV energy shift. However, these calculations were not able to reproduce the shapes of the inelastic angular distributions for ^{58}Ni and ^{208}Pb.

The present ^{9}Be data do not provide evidence for the importance of quadrupole contributions to the elastic scattering. Quite acceptable fits with the Kisslinger potential could be obtained with or without quadrupole corrections. The uncorrected data could be fit with the LPT potential though with a much smaller energy shift than that required for the other targets. It was not possible to obtain a satisfactory fit to the "quadrupole corrected data" with this potential.

Even with the large uncertainties in the ^{9}Be optical potential, none of the DWIA calculations, either microscopic or macroscopic, were able to account for the change in the ratio of the cross sections for $\pi^+$and π^- scattering to the $\frac{7}{2}^-$, 6.8-MeV state in ^{9}Be from ~1.0 at 162 MeV to ~1.8 at 291 MeV. The macroscopic calculations predict $\sigma(\pi^+)/\sigma(\pi^-)\approx 1$ (for the same deformation parameters) and the microscopic calculations predict $\sigma(\pi^+)/\sigma(\pi^-)\approx 2$ at both energies. The change in this ratio may be understood as due to a change in the radial localization of pion reactions with changing bombarding energy. This affects the relative importance of single-particle and collective components of the transition density, and illustrates that pion scattering on resonance is particularly sensitive to surface vibrations.

ACKNOWLEDGMENTS

We acknowledge the cooperation and assistance of the staff of LAMPF and EPICS during the course of this experiment. We also wish to thank K. Thayer and D. Kurth for their help in this work. We are particularly grateful to Dr. T. S. H. Lee and Dr. D. Kurath for the use of their inelastic scattering calculations. This work was performed under the auspices of the U.S. Department of Energy and was supported in part by the National Science Foundation.

*Present address: Department of Physics, Indiana University, Bloomington, Indiana 47401.
†Present address: Department of Physics, University of South Carolina, Columbis, South Carolina 29208.
‡Present address: Laboratorium fur Hochenergiephysik, ETH-Z c/o SIN, Switzerland.

[1]See, for example C. H. Q. Ingram, *Meson-Nuclear Physics—1979 (Houston)*, Proceedings of the 2nd International Topical Conference on Meson-Nuclear Physics, edited by E. V. Hungerford III (AIP, New York, 1979), p. 455 and the references therein.
[2]C. Olmer, D. F. Geesaman, B. Zeidman, S. Chakravarti, T.-S. H. Lee, R. L. Boudrie, R. H. Siemssen, J. F. Amann, C. L. Morris, H. A. Thiessen, G. R. Burleson, M. J. Devereux, R. E. Segel, and L. W. Swenson, Phys. Rev. C 21, 254 (1980).
[3]H. A. Thiessen *et al.* (unpublished).
[4]P. J. Bussey, J. R. Carter, D. R. Dance, D. V. Bugg, A. A. Carter, and A. M. Smith, Nucl. Phys. B58, 363 (1973).
[5]E. Borie, Phys. Lett. 68B, 433 (1977).
[6]J.-F. Germond and C. Wilkin, Phys. Lett. 68B, 229 (1977).
[7]J. S. Blair, *Scattering of Strongly Absorbed Particles*, Boulder Lectures (University of Colorado Press, Boulder, 1966), Vol. 8C, p. 343.
[8]L. S. Kisslinger, Phys. Rev. 98, 761 (1955).
[9]R. Landau, S. Phatak, and F. Tabakin, Ann. Phys. (N.Y.) 78, 299 (1973).
[10]A. W. Thomas and R. H. Landau, Phys. Rep. 58, 123 (1980) and references therein.
[11]D. F. Geesaman, C. Olmer, B. Zeidman, R. L. Boudrie, R. H. Siemssen, J. F. Amann, C. L. Morris, H. A. Thiessen, G. R. Burleson, M. J. Devereux, R. E. Segel, and L. W. Swenson, Phys. Rev. C 18, 2223 (1978).
[12]C. W. DeJager, H. DeVries, and C. DeVries, At. Data Nucl. Data Tables 14, 479 (1974).
[13]M. D. Cooper and R. A. Eisenstein, LASL Report No. LA-6929 MS, 1975 (unpublished).
[14]M. M. Sternheim and E. Auerbach, Phys. Rev. Lett. 25, 1500 (1970).
[15]J. Londegan, K. McVoy, and E. Moniz, Ann. Phys. (N.Y.) 86, 147 (1974).
[16]R. A. Eisenstein and F. Tabakin, Comput. Phys. Commun. 12, 237 (1976).
[17]F. Tabakin, *Meson-Nuclear Physics—1976 (Pittsburgh)*, Proceedings of the International Topical Conference on Meson-Nuclear Physics, edited by P. D. Barnes, R. A. Eisenstein, and L. S. Kisslinger (AIP, New York, 1976), p. 38.
[18]L. C. Liu and C. M. Shakin, Phys. Rev. C 16, 1963 (1977).
[19]M. B. Johnson and D. D. Ernst, Phys. Rev. C 20, 1064 (1979).
[20]E. J. Moniz, I. Sick, R. R. Whitney, J. R. Ficenec, R. D. Kephart, and W. P. Trower, Phys. Rev. Lett. 26, 445 (1971).
[21]G. R. Burleson, G. S. Blanpied, J. Davis, J. S. McCarthy, R. C. Minehart, C. Goulding, C. L. Morris, H. A. Thiessen, W. B. Cottingame, S. Greene, and C. F. Moore, Phys. Rev. C 21, 1452 (1980).
[22]B. M. Preedom, R. Corfu, J.-P. Egger, P. Gretillat, C. Lunke, J. Piffaretti, E. Scharz, J. Jansen, and C. Perrin, Nucl. Phys. A236, 385 (1979).
[23]J. Arvieux, J. P. Albanese, J. Bolger, E. Boschitz, C. H. Q. Ingram, L. Pflug, J. Jansen, J. Zichy, E. Rost, and A. S. Rosenthal, Nucl. Phys. A312, 368 (1978).
[24]R. A. Eisenstein and G. A. Miller, Comput. Phys. Commun. 11, 95 (1976).
[25]T.-S. H. Lee and S. Chakravarti (unpublished).
[26]H.-G. Clerc, K. J. Wetzel, and E. Spamer, Nucl. Phys. A120, 441 (1968).
[27]H. J. Votara, T. A. Clegg, E. J. Ludwig, and W. J. Thompson, Nucl. Phys. A204, 529 (1973).
[28]D. S. Gale and J. S. Eck, Phys. Rev. C 2, 1950 (1973) and references therein.
[29]Y. Horikawa, Y. Torizuka, A. Nakada, S. Mitsunobu, Y. Kojima, and M. Kimura, Phys. Lett. 36B, 9 (1971).
[30]H. Rebel, G. W. Schweiner, G. Schatz, J. Specht, R. Lohken, G. Hauser, D. Habs, and H. Klewe-Nebenow, Nucl. Phys. A182, 145 (1972).
[31]J. Kokame, K. Fukunaja, and H. Nakamura, Phys. Lett. 20, 672 (1966).
[32]D. A. Goldberg, S. M. Smith, H. G. Pugh, P. G. Roos, and N. S. Wall, Phys. Rev. C 7, 1938 (1973).
[33]G. Bruge, J. C. Faive, H. Faraggi, and A. Bussiere, Nucl. Phys. A146, 597 (1970).
[34]M. Inoue, Nucl. Phys. A119, 449 (1965).
[35]M. B. Lewis, Nucl. Data Sheets B5, 243 (1971).
[36]J. S. Blair and I. M. Naqib, Phys. Rev. C 1, 569 (1970).
[37]T.-S. H. Lee and D. Kurath, Phys. Rev. C 21, 293 (1980).
[38]S. Cohen and D. Kurath, Nucl. Phys. 73, 1 (1965).
[39]See AIP document No. PAPS PRVCA 23-2635-31 for 31 pages of tabulations of the pion scattering cross sections reported here. Order by PAPS number and journal reference from American Institute of Physics, Physics Auxiliary Publication Service, 335 E. 45th Street, N. Y., N. Y. 10017. The price is $1.50 for each microfiche, or $5.15 for photocopies. Airmail additional. Make checks payable to the American Institute of Physics.